Identification of novel variations in three cases with rare inherited neuromuscular disorder

WEN-QI CHEN[1-3*], YU-FAN YUAN[2,3*], KE-NA HU[2,3], DONG-LAN SUN[1-3], SI-WEN WANG[1-3], QING-BING HE[4], YAN-MING LIU[5], CONG-YING HAN[5], JING ZHANG[1-3] and YA-ZHOU LI[4]

[1]Prenatal Diagnosis Center, Shijiazhuang Obstetrics and Gynecology Hospital; [2]Hebei Key Laboratory of Maternal and Fetal Medicine; [3]Shijiazhuang Key Laboratory of Reproductive Health, Shijiazhuang, Hebei 050011; [4]Department of Pediatric Orthopaedics, The Third Hospital of Hebei Medical University, Shijiazhuang, Hebei 050051; [5]Prenatal Diagnosis Center, Langfang Maternal and Child Health Care Hospital, Langfang, Hebei 065000, P.R. China

Abstract. Inherited neuromuscular disorder (IND) is a broad-spectrum, clinically diverse group of diseases that are caused due to defects in the neurosystem, muscles and related tissue. Since IND may originate from mutations in hundreds of different genes, the resulting heterogeneity of IND is a great challenge for accurate diagnosis and subsequent management. Three pediatric cases with IND were enrolled in the present study and subjected to a thorough clinical examination. Next, a genetic investigation was conducted using whole-exome sequencing (WES). The suspected variants were validated through Sanger sequencing or quantitative fluorescence PCR assay. A new missense variant of the Spastin (*SPAST*) gene was found and analyzed at the structural level using molecular dynamics (MD) simulations. All three cases presented with respective specific clinical manifestations, which reflected the diversity of IND. WES detected the diagnostic variants in all 3 cases: A compound variation comprising collagen type VI α3 chain (*COL6A3*) (NM_004369; exon19):c.6322G>T(p.E1208*) and a one-copy loss of COL6A3:exon19 in Case 1, which are being reported for the first time; a *de novo SPAST* (NM_014946; exon8):c.1166C>A(p.T389K) variant in Case 2; and a *de novo* Duchenne muscular dystrophy (NM_004006; exon11):c.1150-17_1160delACTTCCTTCTTTGTCAGGGGTACATGATinsC variant in Case 3. The structural and MD analyses revealed that the detected novel *SPAST*: c.1166C>A(p.T389K) variant mainly altered the intramolecular hydrogen bonding status and the protein segment's secondary structure. In conclusion, the present study expanded the IND mutation spectrum. The study not only detailed the precise diagnoses of these cases but also furnished substantial grounds for informed consultations. The approach involving the genetic evaluation strategy using WES for variation screening followed by validation using appropriate methods is beneficial due to the considerable heterogeneity of IND.

Correspondence to: Professor Ya-Zhou Li, Department of Pediatric Orthopaedics, The Third Hospital of Hebei Medical University, 139 Ziqiang Road, Shijiazhuang, Hebei 050051, P.R. China
E-mail: lyz_hbsy@126.com

Dr Jing Zhang, Hebei Key Laboratory of Maternal and Fetal Medicine, 16 Tangubei Road, Shijiazhuang, Hebei 050011, P.R. China
E-mail: zhangjing_hbyd_81@126.com

*Contributed equally

Introduction

Inherited neuromuscular disorder (IND) comprises a large and diverse group of conditions caused by neurosystem, muscle tissue structural and/or functional dysfunction [involving either myofibers or corresponding extracellular matrix (ECM)] and muscle fiber innervation (1). After the etiology of an inherited neuromuscular disorder named Duchenne muscular dystrophy (DMD) was first discovered in 1987 (2), the understanding of the genetic basis of these disorders has markedly progressed, with pathogenic variants on <500 genes detected and reported to be the factors causing neuromuscular diseases (1). Proteins encoded by these genes with pathogenic variants may be associated with skeletal muscles, motor neurons or neuromuscular junctions. In addition, the various diseases caused by the defects in these proteins may have phenotypic overlaps. Consequently, more advanced and potent molecular genetic approaches are needed for precise typing and a conclusive diagnosis (3), which would ultimately be beneficial for follow-up prognostic analysis, genetic counseling and treatment planning. The present study discussed 3 rare and typical cases of these neuromuscular diseases.

Collagen VI-related dystrophies (COL6-RDs) may impair the function of the basal lamina, which is a thin layer of specialized connective tissue surrounding myofibers. COL6-RDs,

which mainly display the features of joint contractures combined with muscle weakness, including diverse overlapped phenotypes, ranging from mild Bethlem muscular dystrophy to severe Ullrich congenital muscular dystrophy. The phenotypes within these two have been referred to as intermediate COL6-RD (4). COL6-RD can be diagnosed based on its typical clinical manifestations and muscle imaging findings together with muscle immunohistochemical analysis results. It is verified by identifying the biallelic or heterozygous pathogenic variant(s) within the collagen type VI α3 chain 1 (*COL6A1*), *COL6A2* or *COL6A3* genes [Mendelian Inheritance in Man (MIM) *120220, *120240 and *120250, respectively] (5-7). COL6-RDs mostly conform to the autosomal dominant (AD) inheritance pattern, with ~50-75% of cases resulting from the *de novo* collagen VI pathogenic variants (8,9). However, COL6-RD cases with an autosomal recessive pattern are also reported and mostly involve nonsense or frameshift variants (10-12). Therefore, it is important to elucidate the clinical and genetic classification of COL6-RD cases for the management of this disease.

Hereditary spastic paraplegia (HSP), another neuromuscular disorder, is a congenital neurodegenerative disorder characterized by dieback corticospinal tract degeneration and axonal swelling, both of which lead to gait deficiency (13). HSP has a prevalence of 1-5 cases per 100,000 individuals. The predominant HSP signs include lower limb spasticity and weakness. HSP is associated with at least 80 genes, and its most common subtype is referred to as spastic paraplegia type IV (SPG4), also known as SPAST-HSP. SPG4 is induced by Spastin (*SPAST*) gene mutations (MIM *604277) (13,14), which accounts for 20 and 40% of simplex HSPs and AD-HSPs, respectively (15-17). SPG4 shows the typical features of insidious progression of gait spasticity in both lower extremities, with more than half of the patients having weak lower extremities together with decreased ankle vibration sense (18). The different onset ages and phenotypic manifestation are the main challenges encountered with SPG4 in clinical practice (19).

Dystrophinopathies represent a wide-spectrum X-linked muscle disease group, including DMD and Becker muscular dystrophy, along with dilated cardiomyopathy related to DMD with increasing severity (20). Of note, the most serious conditions include delayed motor milestones and progressive muscle disorders, which ultimately result in mortality around puberty (21). In ~95% of cases, mutational analysis of the *DMD* gene (MIM *300377) enables a definitive diagnosis (21). Although a variety of novel and promising therapies are on the horizon, with a few having entered clinical trials as well, the treatment approach currently in use is symptomatic treatment. Therefore, genetic diagnosis, screening and counseling become particularly meaningful in this regard.

In the present study, 3 cases with the above neuromuscular disorders were analyzed and diverse genetic and clinical examinations were performed. The clinical phenotypes and genetic variations in these patients are distinctive and worthy of attention.

Materials and methods

Subjects. Approval of the present study was granted by the Ethics Committee of Shijiazhuang Obstetrics and Gynecology Hospital (Shijiazhuang, China; no. 2021-0068).

A total of three cases with myopathy-like symptoms who visited our centers between January 2018 and December 2021 were enrolled in the present study and analyzed retrospectively. A thorough clinical evaluation with/without X-ray imaging and magnetic resonance imaging (MRI) examination was performed. Subsequently, peripheral blood was extracted from the probands and their parents to conduct a genetic evaluation.

Each participant or their guardians as applicable provided written informed consent before participating in the present study. Every participant or their guardians consented to genetic analysis and publication of the results. The protocols of the present study were in line with the Declaration of Helsinki from 1964, its associated amendments and related ethical criteria.

DNA isolation. The genomic DNA (gDNA) was collected in the samples with the QIAamp DNA Blood Mini-Kit (Qiagen GmbH). Thereafter, the quality of the extracted DNA was confirmed on 1% agarose gel using the Qbit DNA Assay Kit in a Qubit 2.0 Fluorometer (Thermo Fisher Scientific, Inc.).

Whole-exome sequencing (WES). WES was conducted according to previous reports (22-24). In brief, the exonic sequences were enriched with the use of the Sure Select Human Exon Sequence Capture Kit (Agilent Technologies, Inc.). Thereafter, Illumina DNA Standards and Primer Premix Kit (Kapa Biosystems; Roche Diagnostics) were employed for quantifying sequencing libraries, which was followed by massively parallel sequencing using the Illumina Novaseq6000 platform (Illumina, Inc.). After sequencing and screening low-quality reads, the high-quality reads (quality level Q30 >89%) were compared against the human reference genome[hg19/GRCh37] using Burrows-Wheeler Aligner tool. The GATK software was then utilized to identify those potential pathogenic variants (https://software.broadinstitute.org/gatk/). The variants in the sample sequences were identified by aligning the sequences against those in the National Center for Bioinformatics (NCBI) database (https://www.ncbi.nlm.nih.gov/) using the 'NCBI Reference Sequence' in Chromas v2.33 (Technelysium Pty Ltd.). In line with the American College of Medical Genetics and Genomics (ACMG) (25) guidelines and related databases [1000 g2015aug_eas (https://www.internationalgenome.org/); ExAC_EAS (http://exac.broadinstitute.org);gnomAD_exome_EAS (http://gnomad.broadinstitute.org/); Human Gene Mutation Database (HGMD) (professional version 2019.4) (hgmd.cf.ac.uk/ac/index); ClinVar (https://www.ncbi.nlm.nih.gov/clinvar/) with the Enliven® Variants Annotation Interpretation system (Berry Genomics)], detected variants were assessed for their pathogenicity. The REVEL score was used to predict the pathogenicity of missense variation.

Variant verification. Verification through Sanger sequencing was carried out using the 3500DX Genetic Analyzer (Applied Biosystems; Thermo Fisher Scientific, Inc.) to validate suspected diagnostic variants. By adopting MEGA7 (http://www.megasoftware.net), the evolutionary conservatism of amino acids was analyzed under the influence of certain missense variants using default parameters.
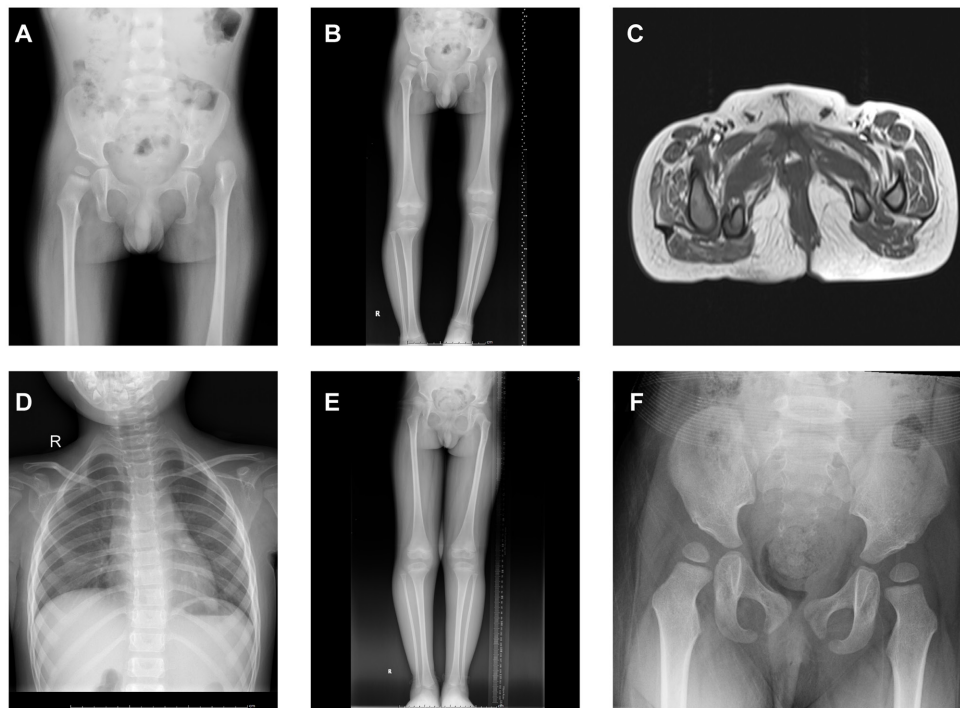
Figure 1. Clinical features of Case 1 and Case 2 in the present study. (A-E) images for Case 1. X-ray indications for (A) left hip dislocation, right hip subluxation and dysplasia of the right acetabulum, and (B) unequal length of the lower limbs. (C) MRI depicting the abnormal signals of the root of the thigh in the center and normal margins. (D) Mild scoliosis (chest X-ray). (E) Healing after the operation (leg X-ray). (F) Image for Case 2 revealing hip joint dysplasia (hip X-ray). According to the wishes of the patient's family, the images of Case 3 were not presented.

To determine the gDNA copy number of the proband and the proband's mother at the variant site in the *COL6A3* gene in Case 1, a set of copy number assays based on quantitative fluorescence PCR (qfPCR) were designed and conducted. Total RNA was extracted from tissue using the RNA kit II (cat. no. R6934; Omega Bio-Tek, Inc.) according to the manufacturer's instructions. The concentration and quality of total RNA were checked using a NanoDrop 2000 spectrophotometer (Thermo Fisher Scientific, Inc.). The first-strand cDNA was synthesized using MonScript™ RTIII Super Mix with dsDNase (two-Step) and oligonucleotide (dT) primers. RT-qPCR analysis of mRNA using the following primers was performed on the ABI 7500 FAST system using TB Green® Premix Ex Taq™ GC (Takara Biotechnology Co., Ltd.). The primers used in this study were as follows: *COL6A3*-exon19 forward, 5'-CCTGTCCGCCTTATT CCCTC-3' and reverse, 3'-AAGGTCACACCTGCTGCAAT-5' (amplicon size, 167 bp) and β-globin forward, 5'-ACACAACTG TGTTCACTAGC-3' and reverse, 3'-CAACTTCATCCACGT TCACC-5' (amplicon size, 110 bp). The PCR conditions were as follows: Initial denaturation at 95˚C for 30 sec, followed by 40 cycles of 10 sec at 95˚C and 30 sec at the annealing temperature of 60˚C. Relative gene expression levels were calculated using the $2^{-\Delta\Delta Cq}$ method (26). The outcome data of the qfPCR were reported as the mean ± standard deviation.

Structural analysis. Wild-type (WT) and spastin: p.T389K mutant models of Spast protein segments were modeled using the Alphafold program (https://alphafold.ebi. ac.uk/entry/E5KRP5). Molecular dynamics (MD) predictions were obtained and analyzed using GROMACS (version 2020.6) (27). MD simulations (60 nsec each) were conducted for the SPAST-WT and SPAST-T389K models. In addition, hydrogen atoms and C- and N-terminal patches were added to the models by applying the CHARMM^{3}6 force field (28). Later mutant or WT protein structures were enclosed within the water-containing cubic box, with a distance of ≥1.0 nm away from box edges. Neutralization was completed using Cl⁻ and Na⁺ ions. MD simulations were performed for a 60-nsec period at 300 K following energy equilibration and minimization. Furthermore, the following GROMACS distribution programs were utilized for generating the MD trajectories: gmxrms, gmxrmsf, gmx gyrate, gmx sasa and gmx hbond. The root-mean-square fluctuation, the radius of gyration, root-mean-square deviation, solvent accessible surface area and hydrogen bond (H-bond) number values were generated.

Statistical analysis. Each experiment was carried out three times. Only representative data are presented. Statistical analysis was completed with Microsoft Excel 2016 (Microsoft Corporation) and GraphPad Prism v.6 (GraphPad Software; Dotmatics). ANOVA (parametric) test was applied in determining significance of difference, followed by Tukey's post hoc multiple comparisons test in the event of a significant result. P<0.05 was considered to indicate statistical significance.

Results

Clinical manifestations and family history
Report of case 1. A male, born to non-consanguineous parents in October 2014, had gait abnormalities appearing since learning to walk. In May 2016, the patient was admitted to the Prenatal Diagnosis Center of Shijiazhuang Obstetrics and
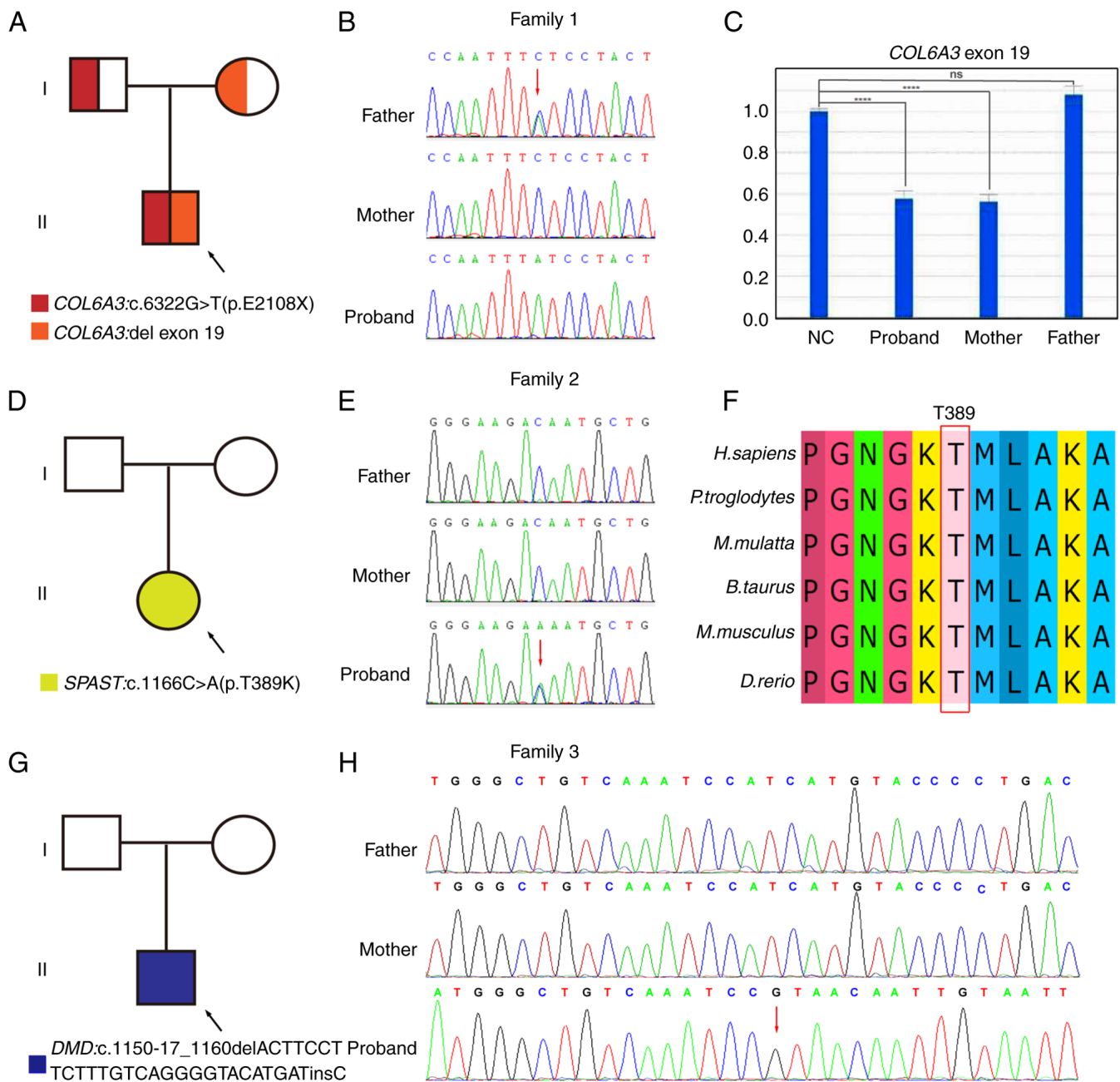
Figure 2. Genetic evaluation findings for the three families in the present study. (A) Pedigree diagram for Family 1. (B) Sanger peak signals of the *COL6A3*: c.6322G>T variant among the members of Family 1. (C) Quantitative fluorescence PCR results for the *COL6A3* exon 19 region spanning c.6322 (****P<0.0001; ns, no significance). (D) The pedigree diagram for Family 2. (E) Sanger peak signals showing the *SPAST*: c.1166C>A variant among the members of Family 2. (F) Conservation of the SPAST: p.T389 amino acid residue among species. (G) The pedigree diagram for Family 3. (H) Sanger peak signals of the *DMD*: c.1150-17_1160delACTTCCTTCTTTGTCAGGGGTACATGATinsC variant in the members of Family 3. The arrows in the pedigree diagrams indicate the probands. NC, negative control; *COL6A3*, collagen type VI α3 chain; *SPAST*, Spastin; *DMD*, Duchenne muscular dystrophy.

Gynecology Hospital for examination. The X-ray revealed 'left hip dislocation, right hip subluxation and dysplasia of the right acetabulum' (Fig. 1A). Physical and X-ray examination revealed slight muscle weakness and unequal length of the lower limbs (Fig. 1B). MRI of the root of the thigh revealed abnormal signals in the center and normal margins (Fig. 1C). With growth, mild scoliosis appeared in the year 2019 (Fig. 1D). In May 2017, incision reduction of left hip dislocation, salter osteotomy of the pelvis and internal fixation of the proximal femur were performed, and the postoperative healing was satisfactory (Fig. 1E). Follow-up until the age of 8 years

revealed that the patient had not developed any respiratory or dermatological symptoms.

Report of case 2. A male, born in September 2017, had been unable to walk since birth. The physical examination conducted in the Prenatal Diagnosis Center of Shijiazhuang Obstetrics and Gynecology Hospital in September 2019 revealed significantly increased muscle tension, poor activity and joint contracture in both lower limbs. X-ray examination demonstrated dysplasia of the hip joints (Fig. 1F). The patient's parents reported cognitive impairment evidenced by intellectual disability, dysfunction of the bladder sphincter evidenced
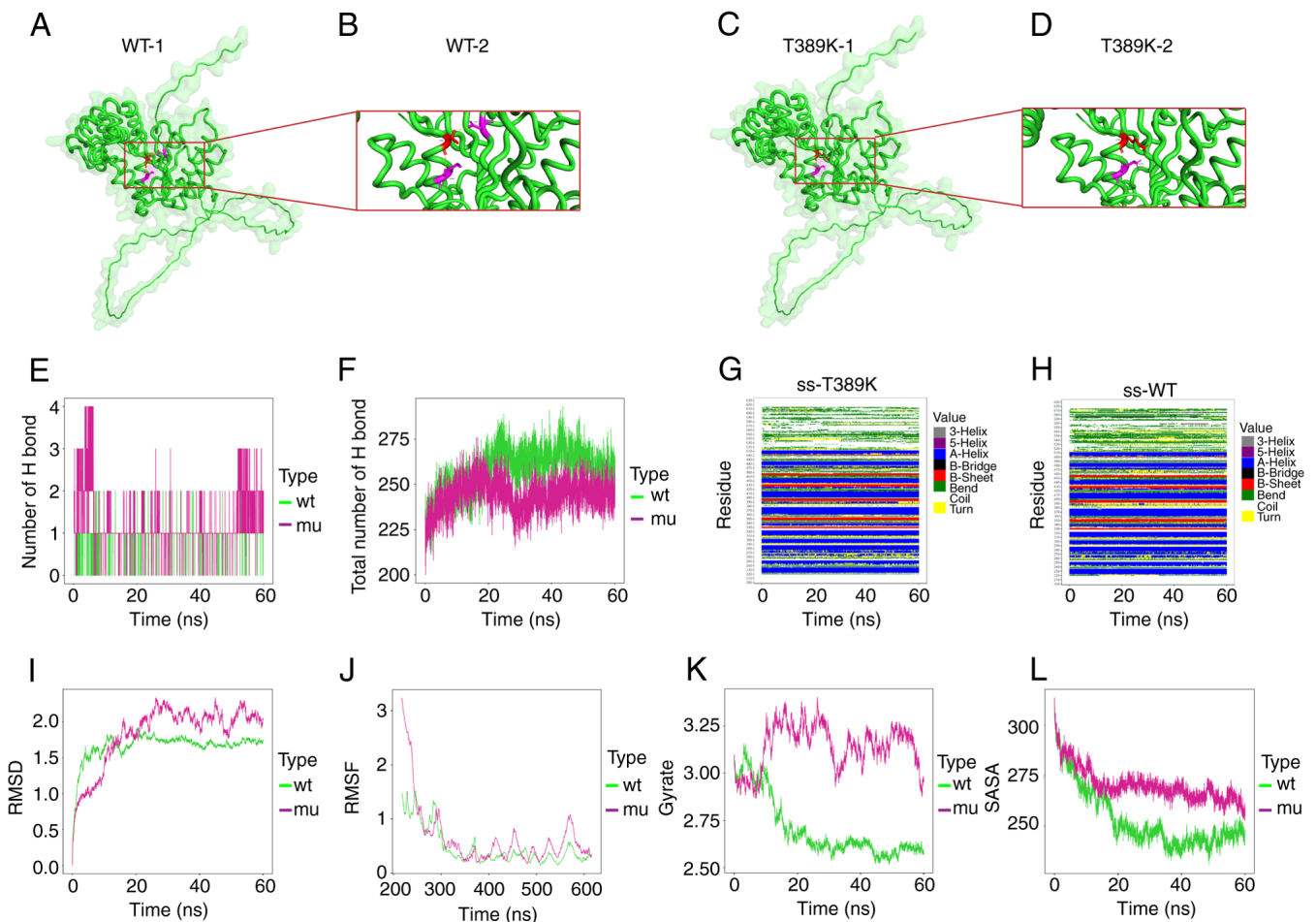
Figure 3. Results of the structure and MD analyses on *SPAST*: c.1166C>A(p.T389K) variation. (A) The WT structure of the SPAST protein and (B) enlarged image of the segment containing the T389 residue. (C) The mutant structure of SPAST protein and (D) enlarged segment containing the variant K389 residue. (E) The H-bond number generated in target amino acid (T389 or K389) and the other residues. (F) The total number of hydrogen bonds in the WT and mutant models, respectively. (G and H) Comparison of the local secondary structure data between (G) the T389K mutant and (H) WT. (I) RMSD: Parameter indicating heterogeneity in the two structures. (J) RMSF: Similar to RMSD, although rather than representing the heterogeneity in the position with time for the entire structure, this measure calculates the flexibility of a single residue or the extent to which one specific residue migrates (fluctuates) in the simulation process. (K) Gyrate: Measure of the structural displacement of a protein atom with its shared mass center during simulation, which offers integrated data regarding protein tightness with time. (L) SASA: Parameter indicating the surface exposed within a protein structure, which can be accessed by the solvent molecules. WT, wild-type; mu, mutant; ns, nanoseconds; SPAST, Spastin; RMSD, root mean square deviation; RMSF, root mean square fluctuation; SASA, solvent accessible surface area.

by urinary urgency and urinary incontinence symptoms in the patient at 2 years old. Continuous follow-up of this case is necessary to see if its recent clinical phenotype is consistent with the clinical diagnosis of SPG4.

Report of case 3. A male, born in August 2017, presented to the Prenatal Diagnosis Center of Shijiazhuang Obstetrics and Gynecology Hospital due to muscle weakness and gait instability. The laboratory evaluation conducted in February 2019 (multiple times) indicated that the patient's serum creatine phosphokinase (CK) concentration was significantly elevated (9-13 times the normal level). A recent follow-up confirmed that the patient frequently experienced an unsteady gait and falls, had a typical presentation of proximal muscle weakness and a high serum CK concentration, although the patient had not yet developed any evident indication of calf hypertrophy. The patient was clinically considered as a case of dystrophinopathy. Calf muscle pseudohypertrophy is the typical clinical feature of dystrophinopathy. Attention should be paid to calf muscle pseudohypertrophy, and dilated cardiomyopathy that

may develop in the proband during development (clinical indication images not presented, as per the wish of the affected family).

Genetic and relative structural findings
Case 1. Fig. 2A displays a pedigree chart along with the carrier status for each variant in this family. The WES detected a homozygous nonsense variation of the *COL6A3* gene-(NM_004369; exon19) c.6322G>T (p.E1208*). According to further Sanger sequencing-based familial verification, the father was heterozygous, while the mother was a WT at this site (Fig. 2B). To provide a clear determination of this special case, a qfPCR-based verification of the *COL6A3* gDNA copy number analysis of the flanking region of this site was performed as described above. The result indicated that both the mother and the proband were heterozygous carriers of a one-copy loss at this region, while the father was WT (Fig. 2C). Accordingly, this proband was ultimately recognized as being affected by a compound heterozygous variation in *COL6A3* comprising one

allelic point mutation and one allelic copy loss, which is being newly reported in the present study.

Case 2. Fig. 2D displays a pedigree diagram along with the carrier status for each variant. WES identified the new missense variant of the *SPAST* gene (NM_014946; exon8) c.1166C>A (p.T389K). Sanger sequencing indicated that this variant was *de novo*, i.e., both of the parents of the proband were WT (Fig. 2E). The MEGA7 result demonstrated that the T389 residue of spastin protein showed a high conservation degree across species (Fig. 2F). To investigate the intramolecular impact resulting from this missense variant, structural analysis and MD simulations were performed. The structural result demonstrated that the T389K variant affected H-bonding within the amino acids inside a protein. Particularly, for the WT, T389 formed H-bonds along with the K393 as well as D441 residues. However, in the T389K mutant, K389 formed an H-bond with K393 (Fig. 3A-D; Fig. 3B and D depict the local amplifications of Fig. 3A and C, respectively). The MD results revealed that the K389 residue in the mutant model generated more H-bonds with other amino acids within that protein in comparison with WT residue T389 (Fig. 3E). In addition, the total number of H-bonds inside the modeled protein segment during 60 nsec was greater in the WT than in the T389K mutant (Fig. 3F). Furthermore, the T389K variant resulted in a change in the secondary structure around the 390th residue (Fig. 3G and H). Specifically, in the WT, the secondary structure at this position alternated between α-helix and TURN, with the domination of TURN. However, in the mutant, the secondary structure alternated between α-helix and TURN, with the domination of α-helix. Finally, the T389K variant resulted in greater changes in the protein structure (Fig. 3I), increased amino acid flexibility in the protein (Fig. 3J), decreased protein compactness (Fig. 3K) and increased surface area accessible to the protein solvent (Fig. 3L).

Case 3. The pedigree diagram and the carrying status of each variant are presented in Fig. 2G. WES identified the following insertion and deletion (InDel) variation in the *DMD* gene: (NM_004006; exon11) c.1150-17_1160delACTTCC TTCTTTGTCAGGGGGTACATGATinsC. Accordingly, it was preliminarily concluded that the mutation would affect the normal splicing of this gene. Familial validation demonstrated that this variation was *de novo* (Fig. 2H).

Table I lists the main clinical and genetic indications of the 3 cases described above.

Discussion

IND attracts much attention in the research field due to its wide variability along with severe clinical impact (29). Although hundreds of disease-causing genes have been identified, only a small number of effective treatments have been developed so far, and more genetic research is necessary, particularly in the area of genotype-phenotype association (30). Whether the knowledge of new mutations could offer potential treatment options requires further investigation. Reporting additional cases associated with these mutations may help identify genotype-phenotype correlations and lead to clinical trials in the future. Although gene therapy has been developed for certain rare genetic diseases, there are still several challenges

Table I. Main clinical and genetic indications of the 3 cases.

Case no.	Sex	Age, years	Major clinical features	Gene	Genomic variation	Peptide alteration	Frequency in three databases[a]	Prediction by REVEL[b]	HGMD/ClinVar[c] rating	Pathogenicity rating[d] (evidence)
1	M	4	Hip dislocation; hip subluxation; acetabulum dysplasia; scoliosis	*COL6A3*	c.6322G>T	p.E2108 X	0; 0; 0	/	/	LP (PVS1+PM2)
				COL6A3	Exonic one-copy loss	Uncertain	0; 0; 0	/	/	LP (PVS1+ PM2+PM3)
2	F	2	Increased muscle tension; poor activity; joint contracture; hip dysplasia	*SPAST*	c.1166C>A	p. T389K	0; 0; 0	D	/	LP (PS2+ PM2+PP3)
3	M	2	Delay of motor development; calf hypertrophy	*DMD*	c.1150-17_1160delACT TCCTTCTTTGTCAG GGGTACATGATinsC	Splicing error	0; 0; 0	/	/	P (PVS+ PS2+PM2)

[a]Databases: 1000g2015aug_eas (https://www.internationalgenome.org/); ExAC_EAS (http://exac.broadinstitute.org/); gnomAD_exome_EAS (http://gnomad.broadinstitute.org/). [b]REVEL: A comprehensive tool for predicting pathogenicity of missense variation (44); HGMD (professional version 2019.4; http://www.hgmd.cf.ac.uk/ac/index.php); ClinVar (https://www.ncbi.nlm.nih.gov/clinvar/); [c]HGMD (professional version 2019.4; http://www.hgmd.cf.ac.uk/ac/index.php). HGMD, Human Gene Mutation Database; *COL6A3*, collagen type VI α3 chain; *SPAST*, Spastin; *DMD*, Duchenne muscular dystrophy; D, damaging; M, male; F, female; LP, likely pathogenic. [d]Pathogenicity rating: Based on the common guideline issued by the American Association of Medical Genetics and Genomics. HGMD, Human Gene Mutation Database; *COL6A3*, collagen type VI α3 chain; *SPAST*, Spastin; *DMD*, Duchenne muscular dystrophy; D, damaging; M, male; F, female; LP, likely pathogenic.

in gene therapy. The first challenge in treating hereditary heterogeneous diseases is to identify the pathogenic genes. New mutations identified in this study are potential targets for future gene therapy. In the present study, 3 cases, including Bethlem muscular dystrophy, AD-HSP and dystrophinopathy, were analyzed clinically and genetically, and their specific features were described. All variants identified in the three cases were divided into pathogenic (P) and likely pathogenic (LP) variants. According to the ACMG criteria (25), the COL6A3:c.6322G>T (p.E1208*) variant was categorized as LP, with the evidence of PVS1+PM2, the SPAST: c.1166C>A (p.T389K) variant was classified as LP, with the evidence of PS2+PM2+PP3, and the *DMD* gene: c.1150-17_1160delACT TCCTTCTTTGTCAGGGGTACATGATinsC variant was categorized as P, with the evidence of PVS1+PS2+PM2.

In Case 1, the initial manifestation of the proband was hip dislocation. The physical examination did not reveal any significant hypotonia or joint contracture. Furthermore, the MRI results were only marginally suggestive. The patient was clinically considered as a case of Bethlem muscular dystrophy. The main clinical features of this disease include joint contractures and respiratory dysfunction caused by muscle weakness.

The follow-up until the age of 8 years demonstrated that the patient had not developed any respiratory or skin involvement thus far. Attention should be paid to muscle weakness, respiratory and dermatological symptoms that may develop in the proband during development. Genetic evaluation with WES initially identified a homozygous *COL6A3* stop-gain variation designated as c.6322G>T (p.E1208*), which was a rare occurrence (10,31). A noteworthy observation in this case, which was consistent with a previous report, was that the pathogenic variants responsible for recessive COL6-RD tended to be nonsense or frameshift variants (12). Interestingly, the proband's father carried the heterozygous variant, while the mother was of the WT, which may allow for the hypothesis that this variation in this patient may have been due to a *de novo* mutation in the oocyte, a uniparental isodisomy, maternal mosaicism (32), or, more likely, maternal copy number loss (4,33,34). A simple qfPCR assay revealed that both the patient and the mother carried one-copy-loss of the *COL6A3*: exon 19 segment. Bethlem muscular dystrophy is caused by mutation in the *COL6A3* gene, and it was inferred that this patient should be clinically classified as a case of mild Bethlem muscular dystrophy. However, due to methodological limitations, the specific breakpoint causing the deletion remained unknown, although it did not influence the subsequent processing. Further verification as to whether the symptoms of the patient in Case 1 are caused by the mutation at this site requires further investigation and the lack of this verification is a limitation of the present study. Genetically, the family continues to have a 25% probability of conceiving another child suffering from this condition. Therefore, evidence-based counseling and fertility guidance must be provided to the parents. In addition, attention should be paid to subsequent symptoms that may develop in the proband during development.

SPAST-HSP (SPG4) covers as many as 40% of all AD-HSP cases (17,35). For the patient in Case 2, clinical indications were consistent with previous reports (13,14,36,37). At the level of large cohort clinical studies, neuroimaging and structural biology, researchers have recently tried to explain some of the hallmarks of SPG4, such as the 'double peaks' of the onset age and substantial phenotypic variability (18,38,39). Parodi *et al* (18) indicated that missense variations and truncated mutations of the *SPAST* gene affected protein function at varying degrees, which may be responsible for the younger age of onset in the former and the older age of onset in the latter. Due to interest in the missense variant *SPAST*: c.1166C>A (p.T389K) detected in Case 2 of the present study, structural analysis was performed. The *SPAST*-encoded Spastin represents the microtubule-severing enzyme combining with and generating internal breaks within the microtubule lattice and is, therefore, being increasingly considered a key modulator of the microtubule cytoskeleton in neuron biology (40). Structurally, microtubule severing is performed mainly in the region between the 228 to 616 residues, and the region between 382 and 389 residues constitutes the ATP binding site, which is exactly where the p.T389K is located (41). According to the results of the structural and MD analyses, the T389K variant most likely significantly affected both local and global H-bond formation, thereby leading to altered protein stability, while also disrupting the desired secondary structure of the protein, disrupting the binding of the protein to ATP. However, this hypothesis requires to be validated through solid evidence from *in vitro* functional experiments.

Dystrophinopathy is probably the most well-studied neuromuscular disease to date, with a prevalence of ~1/3,500 in male newborns and one of the few diseases to reach the gene therapy stage (20). The *DMD* gene is located on chromosome Xp21 and is the only recognized pathogenic gene related to this disease. This gene is known for its large span, diverse mutation types and high proportion of *de novo* variants (42). The association between various *DMD* variants and the specific subtypes of dystrophinopathy, which is referred to as the genotype-phenotype association, has been widely discussed in the literature (43). In Case 3 of the present study, a *de novo* deletion-insertion variant was detected in the proband, which spanned the splice site and involved both exonic and intronic regions. This variant most likely affects the splicing process, although its ultimate effect on protein formation remains to be elucidated and validated. Immunohistochemical analysis of dystrophin in patient tissue and *in vitro* functional study by cell transfection should be performed to understand the role of the variant in the entire process of disease development. The current evidence suggests that this variant is *de novo*, and gonadal mosaicism in the proband's mother cannot be ruled out. Therefore, it is prudent to recommend targeted prenatal diagnosis for any subsequent pregnancies in this family. The same suggested measure applies to Case 2. The multiplex ligation-dependent probe amplification (MLPA) method was not used and is a limitation of the present study. MLPA helps to detect large fragment deletions/duplications (multiple consecutive exon or intron deletions/duplications). However, MLPA may lead to a missed diagnosis of single-exon deletion, micro-deletion, micro-duplication and point variations. In the present study, WES identified an InDel variation in exon 11 of the *DMD* gene. MLPA may have led to a missed diagnosis of this microinsertion and deletion variant.

In conclusion, the present study meticulously indexed the clinical manifestations in three patients, along with the related family members. WES detected the diagnostic variants of the

COL6A3, *SPAST* and *DMD* genes in these three patients. In total, four variations were found and verified. Among all variants, to the best of our knowledge, three were identified for the first time, namely *COL6A3* (NM_004369; exon19): c.6322G>T (p.E2108X) in addition to one-copy loss of *COL6A3*, exon19; SPAST (NM_014946; exon8): c.1166C>A (p.T389K); and *DMD* (NM_004006; exon11): c.1150-17_1160delACTTCC TTCTTTGTCAGGGGTACATGATinsC. The results of the present study contributed to genetically diagnosing IND in three cases. These findings extend the spectrum of mutations and the understanding of the genotype-phenotypic associations in these diseases.

Availability of data and materials

The sequencing data generated in the present study may be found in the Figshare repository at the following URLs: [COL6A3 (https://figshare.com/articles/dataset/COL6A3_ NM_004369_exon19_c_6322G_T_p_E1208_/21548523); SPAST (https://figshare.com/articles/dataset/SPAST_NM_014946_ exon8_c_1166C_A_p_T389K_/21548727); and DMD (https://figshare.com/articles/dataset/WES_identified_an_InDel_ insertion_and_deletion_variation_in_the_DMD_gene/21548733)]. The other data generated in the present study are included in the figures and/or tables of this article.

Authors' contributions

YZL and JZ made substantial contributions to conception and design. WQC and YFY were involved in drafting the manuscript and performed the statistical analysis. KNH, DLS and QBH performed the experiments and agreed to be accountable for all aspects of the work in ensuring that questions related to the accuracy were investigated and resolved. SWW, YML and CYH were involved in revising the manuscript critically for important intellectual content and analyzed the data. YZL gave final approval of the version to be published. All authors have read and approved the final version of the manuscript. YZL and JZ confirm the authenticity of all the raw data.

Ethics approval and consent to participate

The current study was approved by the Ethics Committee in Shijiazhuang Obstetrics and Gynecology Hospital (Shijiazhuang, China; approval no. 2021-0068). Each subject or the corresponding guardian provided informed consent before participating in this work. Every participant or their guardians consented to genetic analysis and publication of the results. Every procedure was conducted in accordance with the Declaration of Helsinki from 1964, related amendments and associated ethical guidelines.

Patient consent for publication

Each subject or corresponding guardian provided informed consent for publication of patient information, genetic data and images in this manuscript. Clinical indication images are not presented for case 3, as per the wish of the affected family.

Competing interests

The authors declare that they have no competing interests.

References

1. Dowling JJ, Weihl CC and Spencer MJ: Molecular and cellular basis of genetically inherited skeletal muscle disorders. Nat Rev Mol Cell Biol 22: 713-732, 2021.
2. Koenig M, Hoffman EP, Bertelson CJ, Monaco AP, Feener C and Kunkel LM: Complete cloning of the Duchenne muscular dystrophy (DMD) cDNA and preliminary genomic organization of the DMD gene in normal and affected individuals. Cell 50: 509-517, 1987.
3. Butterfield RJ: Congenital muscular dystrophy and congenital myopathy. Continuum (Minneap Minn) 25: 1640-1661, 2019.
4. Foley AR, Mohassel P, Donkervoort S, Bolduc V and Bönnemann CG: Collagen VI-related dystrophies. In: GeneReviews® [Internet]. Adam MP, Feldman J, Mirzaa GM, Pagon RA, Wallace SE, Bean LH, Gripp KW and Amemiya A (eds). University of Washington, Seattle, WA, 1993.
5. Pepea G, Bertini E, Bonaldo P, Bushby K, Giusti B, de Visser M, Guicheney P, Lattanzi G, Merlini L, Muntoni F, *et al*: Bethlem myopathy (BETHLEM) and Ullrich scleroatonic muscular dystrophy: 100th ENMC international workshop, 23-24 November 2001, Naarden, The Netherlands. Neuromuscul Disord 12: 984-993, 2002.
6. Briñas L, Richard P, Quijano-Roy S, Gartioux C, Ledeuil C, Lacène E, Makri S, Ferreiro A, Maugenre S, Topaloglu H, *et al*: Early onset collagen VI myopathies: Genetic and clinical correlations. Ann Neurol 68: 511-520, 2010.
7. Bönnemann CG: The collagen VI-related myopathies: Muscle meets its matrix. Nat Rev Neurol 7: 379-390, 2011.
8. Allamand V, Merlini L and Bushby K; Consortium for Collagen VI-Related Myopathies: 166th ENMC international workshop on collagen type VI-related myopathies, 22-24 May 2009, Naarden, The Netherlands. Neuromuscul Disord 20: 346-354, 2010.
9. Allamand V, Briñas L, Richard P, Stojkovic T, Quijano-Roy S and Bonne G: ColVI myopathies: Where do we stand, where do we go? Skelet Muscle 1: 30, 2011.
10. Foley AR, Hu Y, Zou Y, Columbus A, Shoffner J, Dunn DM, Weiss RB and Bönnemann CG: Autosomal recessive inheritance of classic Bethlem myopathy. Neuromuscul Disord 19: 813-817, 2009.
11. Zamurs LK, Idoate MA, Hanssen E, Gomez-Ibañez A, Pastor P and Lamandé SR: Aberrant mitochondria in a Bethlem myopathy patient with a homozygous amino acid substitution that destabilizes the collagen VI α2(VI) chain. J Biol Chem 290: 4272-4281, 2015.
12. Camacho Vanegas O, Bertini E, Zhang RZ, Petrini S, Minosse C, Sabatelli P, Giusti B, Chu ML and Pepe G: Ullrich scleroatonic muscular dystrophy is caused by recessive mutations in collagen type VI. Proc Natl Acad Sci USA 98: 7516-7521, 2001.
13. Hedera P: Hereditary spastic paraplegia overview. In: GeneReviews® [Internet]. Adam MP, Feldman J, Mirzaa GM, Pagon RA, Wallace SE, Bean LJ, Gripp KW and Amemiya A (eds). University of Washington, Seattle, WA, 1993.
14. Parodi L, Rydning SL, Tallaksen C and Durr A: Spastic paraplegia 4. In: GeneReviews® [Internet]. Adam MP, Feldman J, Mirzaa GM, Pagon RA, Wallace SE, Bean LJ, Gripp KW and Amemiya A (eds). University of Washington, Seattle, WA, 1993.

15. Erichsen AK, Koht J, Stray-Pedersen A, Abdelnoor M and Tallaksen CM: Prevalence of hereditary ataxia and spastic paraplegia in southeast Norway: A population-based study. Brain 132: 1577-1588, 2009.
16. Fei QZ, Tang WG, Rong TY, Tang HD, Liu JR, Guo ZL, Fu Y, Xiao Q, Wang XJ, He SB, *et al*: Two novel mutations in the Spastin gene of Chinese patients with hereditary spastic paraplegia. Eur J Neurol 18: 1194-1196, 2011.
17. Ruano L, Melo C, Silva MC and Coutinho P: The global epidemiology of hereditary ataxia and spastic paraplegia: A systematic review of prevalence studies. Neuroepidemiology 42: 174-183, 2014.
18. Parodi L, Fenu S, Barbier M, Banneau G, Duyckaerts C, Tezenas du Montcel S, Monin ML, Ait Said S, Guegan J, Tallaksen CME, *et al*: Spastic paraplegia due to SPAST mutations is modified by the underlying mutation and sex. Brain 141: 3331-3342, 2018.
19. Méreaux JL, Banneau G, Papin M, Coarelli G, Valter R, Raymond L, Kol B, Ariste O, Parodi L, Tissier L, *et al*: Clinical and genetic spectra of 1550 index patients with hereditary spastic paraplegia. Brain 145: 1029-1037, 2022.
20. Darras BT, Urion DK and Ghosh PS: Dystrophinopathies. 2000 Sep 5 (Updated 2022 Jan 20). In: Adam MP, Feldman J, Mirzaa GM, Pagon RA, Wallace SE, Bean LJ, Gripp KW and Amemiya A (eds). GeneReviews® [Internet]. Seattle (WA): University of Washington, Seattle, 1993.
21. Flanigan KM: Duchenne and Becker muscular dystrophies. Neurol Clin 32: 671-688, viii, 2014.
22. Zhang J, Hu H, Mu W, Yu M, Chen W, Mi D, Yang K and Guo Q: Case report: Exome sequencing identified a novel compound heterozygous variation in PLOD2 causing bruck syndrome type 2. Front Genet 12: 619948, 2021.
23. Huang YX, Gao CY, Zheng CY, Chen X, Yan YS, Sun YQ, Dong XY, Yang K and Zhang DL: Investigation of a novel LRP6 variant causing autosomal-dominant tooth agenesis. Front Genet 12: 688241, 2021.
24. Yang F, Yang RJ, Li Q, Zhang J, Meng YX, Liu XJ and Yao YF: Whole-exome sequencing facilitates the differential diagnosis of Ehlers-Danlos syndrome (EDS). Mol Genet Genomic Med 10: e1885, 2022.
25. Richards S, Aziz N, Bale S, Bick D, Das S, Gastier-Foster J, Grody WW, Hegde M, Lyon E, Spector E, *et al*: Standards and guidelines for the interpretation of sequence variants: A joint consensus recommendation of the American college of medical genetics and genomics and the association for molecular pathology. Genet Med 17: 405-424, 2015.
26. Livak KJ and Schmittgen TD: Analysis of relative gene expression data using real-time quantitative PCR and the 2(-Delta Delta C(T)) method. Methods 25: 402-408, 2001.
27. Rakhshani H, Dehghanian E and Rahati A: Enhanced GROMACS: Toward a better numerical simulation framework. J Mol Model 25: 355, 2019.
28. Soteras Gutiérrez I, Lin FY, Vanommeslaeghe K, Lemkul JA, Armacost KA, Brooks CL III and MacKerell AD Jr: Parametrization of halogen bonds in the CHARMM general force field: Improved treatment of ligand-protein interactions. Bioorg Med Chem 24: 4812-4825, 2016.
29. Pelin K and Wallgren-Pettersson C: Update on the genetics of congenital myopathies. Semin Pediatr Neurol 29: 12-22, 2019.
30. Scoto M, Finkel R, Mercuri E and Muntoni F: Genetic therapies for inherited neuromuscular disorders. Lancet Child Adolesc Health 2: 600-609, 2018.
31. Gualandi F, Urciuolo A, Martoni E, Sabatelli P, Squarzoni S, Bovolenta M, Messina S, Mercuri E, Franchella A, Ferlini A, *et al*: Autosomal recessive Bethlem myopathy. Neurology 73: 1883-1891, 2009.
32. Armaroli A, Trabanelli C, Scotton C, Venturoli A, Selvatici R, Brisca G, Merlini L, Bruno C, Ferlini A and Gualandi F: Paternal germline mosaicism in collagen VI related myopathies. Eur J Paediatr Neurol 19: 533-536, 2015.
33. Chen GL and Li DZ: Germline mosaicism in a collagen VI-related myopathy family: A cause of autosomal recessive inheritance. Congenit Anom (Kyoto) 61: 197-198, 2021.
34. Inoue M, Saito Y, Yonekawa T, Ogawa M, Iida A, Nishino I and Noguchi S: Causative variant profile of collagen VI-related dystrophy in Japan. Orphanet J Rare Dis 16: 284, 2021.
35. Varghaei P, Estiar MA, Ashtiani S, Veyron S, Mufti K, Leveille E, Yu E, Spiegelman D, Rioux MF, Yoon G, *et al*: Genetic, structural and clinical analysis of spastic paraplegia 4. Parkinsonism Relat Disord 98: 62-69, 2022.
36. Orlacchio A, Kawarai T, Totaro A, Errico A, St George-Hyslop PH, Rugarli EI and Bernardi G: Hereditary spastic paraplegia: Clinical genetic study of 15 families. Arch Neurol 61: 849-855, 2004.
37. Giordani GM, Diniz F, Fussiger H, Gonzalez-Salazar C, Donis KC, Freua F, Ortega RPM, de Freitas JL, Barsottini OGP, Rosemberg S, *et al*: Clinical and molecular characterization of a large cohort of childhood onset hereditary spastic paraplegias. Sci Rep 11: 22248, 2021.
38. Piermarini E, Akarsu S, Connors T, Kneussel M, Lane MA, Morfini G, Karabay A, Baas PW and Qiang L: Modeling gain-of-function and loss-of-function components of SPAST-based hereditary spastic paraplegia using transgenic mice. Hum Mol Genet 31: 1844-1859, 2022.
39. Karle KN, Schüle R, Klebe S, Otto S, Frischholz C, Liepelt-Scarfone I and Schöls L: Electrophysiological characterisation of motor and sensory tracts in patients with hereditary spastic paraplegia (HSP). Orphanet J Rare Dis 8: 158, 2013.
40. Costa AC and Sousa MM: The role of spastin in axon biology. Front Cell Dev Biol 10: 934522, 2022.
41. Liu Q, Zhang G, Ji Z and Lin H: Molecular and cellular mechanisms of spastin in neural development and disease (Review). Int J Mol Med 48: 218, 2021.
42. Aartsma-Rus A, Van Deutekom JC, Fokkema IF, Van Ommen GJ and Den Dunnen JT: Entries in the Leiden Duchenne muscular dystrophy mutation database: An overview of mutation types and paradoxical cases that confirm the reading-frame rule. Muscle Nerve 34: 135-144, 2006.
43. Monaco AP, Bertelson CJ, Liechti-Gallati S, Moser H and Kunkel LM: An explanation for the phenotypic differences between patients bearing partial deletions of the DMD locus. Genomics 2: 90-95, 1988.
44. Ioannidis NM, Rothstein JH, Pejaver V, Middha S, McDonnell SK, Baheti S, Musolf A, Li Q, Holzinger E, Karyadi D, *et al*: REVEL: An ensemble method for predicting the pathogenicity of rare missense variants. Am J Hum Genet 99: 877-885, 2016.